Wireless Netw (2011) 17:685–699
DOI 10.1007/s11276-010-0307-6

Design of MAC-defined aggregated ARQ schemes for IEEE 802.11n networks

Kai-Ten Feng · Yu-Zhi Huang · Jia-Shi Lin

Published online: 15 December 2010

Abstract Based on the IEEE 802.11n standard, frame aggregation is considered one of the major factors to improve system performance of wireless local area networks (WLANs) from the medium access control (MAC) perspective. In order to fulfill the requirements of high throughput performance, feasible design of automatic repeat request (ARQ) mechanisms becomes important for providing reliable data transmission. In this paper, two MAC-defined ARQ schemes are proposed to consider the effect of frame aggregation for the enhancement of network throughput. An aggregated selective repeat ARQ (ASR-ARQ) algorithm is proposed, which incorporates the conventional selective repeat ARQ scheme with the consideration of frame aggregation. On the other hand, the aggregated hybrid ARQ (AH-ARQ) protocol is proposed to further enhance throughput performance by adopting the Reed-Solomon block code as the forward error correction (FEC) scheme. Novel analytical models based on the signal flow graph are established in order to realize the retransmission behaviors of both schemes. Simulations are conducted to validate and compare the proposed ARQ mechanisms with existing schemes based on service time distribution. Numerical results show that the proposed AH-ARQ protocol outperforms the other retransmission schemes owing to its effective utilization of FEC mechanism.

K.-T. Feng (✉) · Y.-Z. Huang · J.-S. Lin
Department of Electrical Engineering, National Chiao Tung University, Hsinchu, Taiwan
e-mail: ktfeng@mail.nctu.edu.tw

Y.-Z. Huang
e-mail: knight.cm95g@nctu.edu.tw

J.-S. Lin
e-mail: uxoxox.cm96g@g2.nctu.edu.tw

Keywords Wireless local area networks (WLAN) · IEEE 802.11n standard · Medium access control (MAC) · Automatic repeat request (ARQ) · Performance analysis

1 Introduction

In recent years, the techniques for wireless local area networks (WLANs) have been prevailing exploited for both indoor and mobile communications. The applications for WLANs include wireless home gateways, hotspots for commercial usages, and ad-hoc networking for inter-vehicular communications. Among different techniques, the IEEE 802.11 standard is considered the well-adopted suite due to its remarkable success in both design and deployment. Various amendments are contained in the IEEE 802.11 standard suite, mainly including IEEE 802.11a/b/g [1–3] and IEEE 802.11e [4] for quality-of-service (QoS) support.

With increasing demands to support multimedia applications, the new amendment IEEE 802.11n [5, 6] has been proposed for achieving high throughput performance. The IEEE 802.11 task group N (TGn) enhances the PHY layer data rate up to 600 Mbps by adopting advanced communication techniques, such as multi-input multi-output (MIMO) technology [7]. It is noted that the MIMO technique utilizes spatial diversity to improve both the range and spatial multiplexing for achieving higher data rate. However, it has been investigated in [8] that simply improves the PHY data rate will not be sufficient for enhancing the system throughput from the medium access control (MAC) perspective. Accordingly, the IEEE 802.11 TGn further exploits frame aggregation and block acknowledgement techniques [6, 9] to moderate the drawbacks that are originated from the MAC/PHY overheads.

The benefits of adopting frame aggregation techniques have been studied from different perspectives [9–12]. Without the consideration of retransmission mechanisms, simplified performance analysis considering frame aggregation has been conducted in [10] based on channel utilization. The dynamic frame aggregation scheme [11] adaptively changes the number of aggregated frames based on the channel conditions. Moreover, the multi-user polling controlled channel access (MCCA) protocol [12] performs both frame aggregation and multi-user polling in order to further enhance network utilization. Although the frame aggregation techniques can reduce both the transmission time of frame headers and the contention time induced by the random backoff period, the enlarged aggregated frames will cause other wireless stations to wait for an elongated time period before their next opportunity for channel access. Furthermore, under the error-prone channels, corrupting an aggregated frame can result in the wastage of a longer channel access period which consequently leads to inferior throughput performance. Therefore, a feasible design of retransmission mechanisms becomes an important topic with the adoption of frame aggregation scheme.

The automatic repeat request (ARQ) [13–15] mechanisms have been extensively proposed in different wireless systems for reliable transmission. In order to reach more reliable transmissions within a shorter transmitting period, the hybrid ARQ (H-ARQ) schemes [16–20], which combine both the forward error correction (FEC) and retransmission mechanism, have been proposed for advanced multimedia applications. In general, the H-ARQ algorithms can be classified into three categories as follows. In the type-I H-ARQ scheme [18], as an error packet is detected via the cyclic redundancy check, the transmitter will retransmit the same packet either until the packet is successfully decoded at the receiver or a maximum retransmission limit is reached. Type-II of H-ARQ scheme is regarded as the full incremental redundancy (IR) technique [19], which decreases the coding rate in each retransmission by sending additional redundancy check digits. On the other hand, type-III of H-ARQ scheme [20], considered as a partial IR scheme, not only decrements the coding rate but also maintains the self-decoding capability in each retransmission. It is noted that the IR-based algorithms in general make use of either the rate compatible punctured convolutional (RCPC) codes [20, 21] or the rate compatible punctured turbo (RCPT) codes [22]. Furthermore, the transmission errors are corrected in two phases based on the design concept of concatenate code [23]. The inner decoder, which is implemented in the PHY layer, adopts sophisticated algorithms for error correction; while the outer decoder is served as the second stage fine-tuning error corrector that is implemented in the MAC layer protocols. As a consequence, the FEC schemes in both type-II and III of H-ARQ algorithms are regarded as the inner decoders; while that of type-I scheme is considered as the outer decoders.

However, most of the existing ARQ algorithms did not explicitly consider the effects from frame aggregation. Even though ARQ scheme is utilized for multi-frame retransmission such as in [11], its design concept is primarily based on a pure stop-and-wait ARQ (SW-ARQ) mechanism. It is required to provide an efficient retransmission scheme in order to enhance the system throughput for the IEEE 802.11n networks. In this paper, MAC-defined ARQ mechanisms are proposed to consider the effect from frame aggregation in order to improve the network throughput. An aggregated selective repeat ARQ (ASR-ARQ) algorithm is proposed which incorporates the conventional selective repeat ARQ scheme with the consideration of frame aggregation. On the other hand, an aggregated hybrid ARQ (AH-ARQ) mechanism is proposed to further enhance the throughput performance for the IEEE 802.11n networks. The proposed AH-ARQ scheme can be categorized as type-I of H-ARQ algorithm, which is served as an outer code designed from the MAC layer perspective. The Reed-Solomon (RS) code [24, 25], which defines a finite codeword length, is adopted within the AH-ARQ scheme.

Furthermore, it will be beneficial to construct effective analytical models to evaluate the retransmission mechanisms for the IEEE 802.11n networks. There are existing studies that propose analytical models for performance evaluation of the MAC channel access [26–28] and frame aggregation techniques [29–31] in the IEEE 802.11-based networks. However, none of these models explicitly considers efficient retransmission schemes that are especially feasible for high throughput requirements. As a consequence, the analytical models for the service time distribution are constructed in order to observe the behaviors of both the ASR-ARQ and AH-ARQ algorithms. A novel approach based on the signal flow graph is utilized for the construction of analytical models for both schemes. Simulations are performed to both validate and compare the proposed ARQ schemes with conventional mechanism. It will be shown in the numerical results that the AH-ARQ algorithm outperforms the other schemes due to its efficient utilization of FEC mechanism.

The remainder of this paper is organized as follows. Section 2 describes the frame aggregation mechanism of IEEE 802.11n standard and the proposed ARQ algorithms. The system modeling and performance analysis of proposed ARQ schemes are addressed in Sect. 3. Section 4 provides the performance evaluation; while the conclusions are drawn in Sect. 5.

2 Proposed MAC-defined aggregated ARQ schemes

In this section, the frame aggregation structure defined in the IEEE 802.11n MAC protocol is reviewed in Subsect. 2.1. The proposed ASR-ARQ and AH-ARQ protocols are explained in Subsects. 2.2 and 2.3, respectively.

2.1 Frame aggregation/de-aggregation of IEEE 802.11n MAC protocol

The IEEE 802.11n standard mandates the implementation of frame aggregation scheme for the sake of promoting transmission efficiency. It is noted that the transmission efficiency is defined as the time for delivering the information payload over the time duration for transmitting the entire aggregated frame associated with the required control frames and contention periods. With the frame aggregation scheme as shown in Fig. 1, multiple MAC protocol data units (MPDUs) are combined into an aggregated MPDU (A-MPDU), which is consequently transported into a single PHY service data unit (PSDU). Intuitively, the transmission efficiency can be improved with the utilization of A-MPDU since more MPDUs are transmitted with a common control overhead.

Each MPDU is padded with an MPDU delimiter for the purpose of extracting the corresponding MPDU from the aggregated frame. The extracting delimiter is composed of four bytes as shown in Fig. 1, including the reserved, MPDU length, cyclic redundancy check (CRC), and unique pattern (UP) fields. It is noted that the UP field, which is set to the ASCII value of character 'N', is employed to detect the location of an MPDU delimiter while scanning within the aggregated frame. Moreover, each MPDU is padded to become a multiple of four octets as shown in Fig. 1. The de-aggregation procedure at the receiver side described in the standard is rewritten into pseudo-code as shown in Algorithm 1. The receiver verifies the validity of MPDU delimiter via the valid_MPDU_Delimiter function (in Algorithm 1) based on the 8-bits CRC and the observation of UP field, i.e. to exam the correctness of character 'N'. An MPDU can be successfully extracted from the A-MPDU if the corresponding MPDU delimiter is found to be valid. The de-aggregation process will continue to move forward with four bytes, i.e. via the offset parameter in Algorithm 1, and to verify if the next multiple of four octets contains a valid delimiter.

```
offset = 0 ;
while offset+4 ≤ A_MPDU_length do
    length = get_MPDU_length(offset) ;
    if [valid_MPDU_Delimiter(offset)] = True & [0 < length ≤ max_MPDU_length] =
    True then
        receive_MPDU(offset + 4, length) ;
        offset = offset + 4 ∗⌈ (length + 4)/4 ⌉ ;
    end
    else
        offset = offset + 4 ;
    end
end
```

2.2 Proposed aggregated selective repeat (ASR) ARQ scheme

The design of retransmission mechanisms is an open topic from the standpoint of IEEE 802.11n standard. In this paper, the proposed ASR-ARQ scheme is enhanced from conventional selective repeat ARQ mechanism to consider frame aggregation within the design of retransmission algorithm. Contributing from the availability of block acknowledgement (BA) scheme within the IEEE 802.11n standard, the ASR-ARQ algorithm can be effectively designed to provide transmission efficiency. Instead of sending individual acknowledgement (ACK) frame, the receiver replies with a BA frame for acknowledging the entire A-MPDU that is initiated from the transmitter. The BA frame consists of 32 octets which contains a bitmap field. Each bit within the bitmap field identifies whether the corresponding MPDU from the aggregated frame has been correctly received. As a consequence, a single BA frame can reduce the control overheads that are required by conventional design, which replies multiple ACK frames in response to an aggregated data frame.

In the proposed ASR-ARQ scheme, each MPDU within an A-MPDU is identified via a unique sequence number as the aggregated frame is transmitted. In the case that some of the MPDUs within an A-MPDU are missing during the transmission, the ASR-ARQ algorithm will continue to

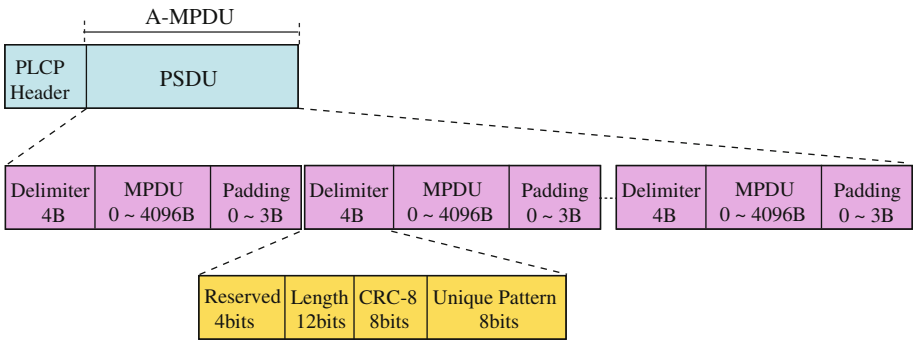

Fig. 1 The A-MPDU frame format from frame aggregation

retransmit those unsuccessfully transmitted MPDUs until all the MPDUs have either been positively acknowledged by the BA frame or reached the retry limitation. For instance, there are N_m MPDUs contained within an A-MPDU that are identified by the sequence numbers from 1 to N_m. If the MPDUs with sequence numbers 3 and 5 are corrupted and are identified via the CRC check, the receiver will reply with the BA frame which denotes two zero flags at the corresponding third and fifth bits within the bitmap field. A new A-MPDU, which includes only the third and fifth MPDUs, will be delivered by the transmitter at the next transmission opportunity. The retransmission procedure terminates until either all the MPDUs with sequence numbers from 1 to N_m are correctly accepted by the receiver or the maximum number of retransmission trials (i.e. identified by the Retry_Limit parameter) has achieved.

2.3 Proposed aggregated hybrid (AH) ARQ scheme

In order to further enhance the transmission efficiency, the AH-ARQ scheme is proposed in this paper to integrate both the RS-based FEC scheme and frame-aggregated retransmission mechanism, which are described in the next two subsections.

2.3.1 FEC mechanism of AH-ARQ scheme

With the compliance to existing IEEE 802.11n MAC frame structure, the proposed FEC mechanism is constructed according to the RS code [24, 25] that is well-adopted in the design of outer decoders. The coefficients of generator polynomial $G(x)$ are elements in a finite field $GF(2^{n_b})$, where $n_b = 8$ is chosen according to the byte-oriented system. For a (n_c, n_i, τ) RS code with $n_c = 2^{n_b} - 1$ as the codeword length, $n_i = 223$ as the size of original information symbols, and τ as the number of corrupted symbols, the set of roots $\boldsymbol{\alpha} = \{\alpha, \alpha^2, \ldots, \alpha^{2\tau}\}$ of $G(x)$ is selected from $GF(2^8)$ where α is a primitive element of the finite field. As a result, the generator polynomial $G(x)$ can be represented as $G(x) = \prod_{i=1}^{2\tau}(x + \alpha^i) = x^{2\tau} + \sum_{i=0}^{2\tau-1} g_i x^i$ with g_i representing the coefficients for all $i \in \{0, \ldots, 2\tau - 1\}$. Based on the cyclic property of RS code, the set of codewords can be formed with the multiplication of both $G(x)$ and the information symbol polynomial $I(x)$. Moreover, the RS code will have the minimum codeword distance $d_{min} \geq 2\tau + 1$ in the case that all the coefficients g_i are not equal to zero. Therefore, the corresponding RS code possesses the correcting capability of τ error symbols associated with the codeword length of n_c octets and n_i information octets. There are total of $n_c - n_i = 2\tau$ parity check octets, which are served as the remainder $R(x)$ while dividing $x^{2\tau}I(x)$ by the generator polynomial $G(x)$.

In order to extract the newly defined MPDU that includes the FEC mechanism, a modified de-aggregation procedure is performed as shown in Algorithm 2. At the beginning, the scanning process will start to search for the UP field. After the UP has been identified, a predefined symbol will be traversed in order to verify the usage of FEC scheme. In other words, a valid delimiter will be identified if the recovered reserved field within the delimiter matches the ASCII value of character FF. After the de-aggregation process has been defined, the entire mechanism for the receiver to manage the incoming A-MPDU is explained as follows. The receiver will first start to extract each MPDU within an A-MPDU as shown in Algorithm 2. In the case that the receiver successfully extracts an MPDU and observes that the corresponding outer FCS is correct, the receiver will enable the corresponding bits within the bitmap field of BA frame. On the other hand, if the outer FCS of corresponding MPDU is incorrect, the receiver will execute the RS decoder in order to decode the RS block in the MAC header. It is noted that the Berlekamp's iterative algorithm [32] is adopted to implement the decoding procedure. If either the decoding process fails or invalid inner FCS of the MAC header's RS block occurs, the process will be terminated by disabling the corresponding bits within the bitmap field of BA frame. On the other hand, if the receiver successfully decodes the MAC header's RS block, it will continue to decode the entire MPDU via the RS decoder. The receiver will set the corresponding bits within the bitmap field of BA frame according to the above results. Consequently, the receiver will send the BA frame back to the transmitter if it has successfully extracted each MPDU from the A-MPDU.

```
offset = 0 ;
while offset + 4 + 2τ ≤ A_MPDU_length do
    length = get_MPDU_length(offset) ;
    if success_decode_Delimiter(offset, offset + 4) then
        if [valid_FCS_check(offset)] = True & [get_reserved_bits(offset)=FF] = True &
        [length ≤ max_MPDU_length] = True then
            RS_decode_MPDU(offset + 4 + 2τ, length);
            offset = offset + 4*⌈(4 + 2τ + length)/4⌉ ;
        end
        else
            offset = offset + 4;
        end
    end
    else
        if [valid_FCS_check(offset)] = True & [length ≤ max_MPDU_length] = True then
            normal_recv_MPDU(offset + 4, length) ;
            offset = offset + 4*⌈(length + 4)/4⌉ ;
        end
        else
            offset = offset + 4;
        end
    end
end
```

2.3.2 Retransmission mechanism of AH-ARQ scheme

The flow diagram for the retransmission mechanism of proposed AH-ARQ scheme is depicted in Fig. 2. It is noted that the main concept of AH-ARQ's retransmission scheme

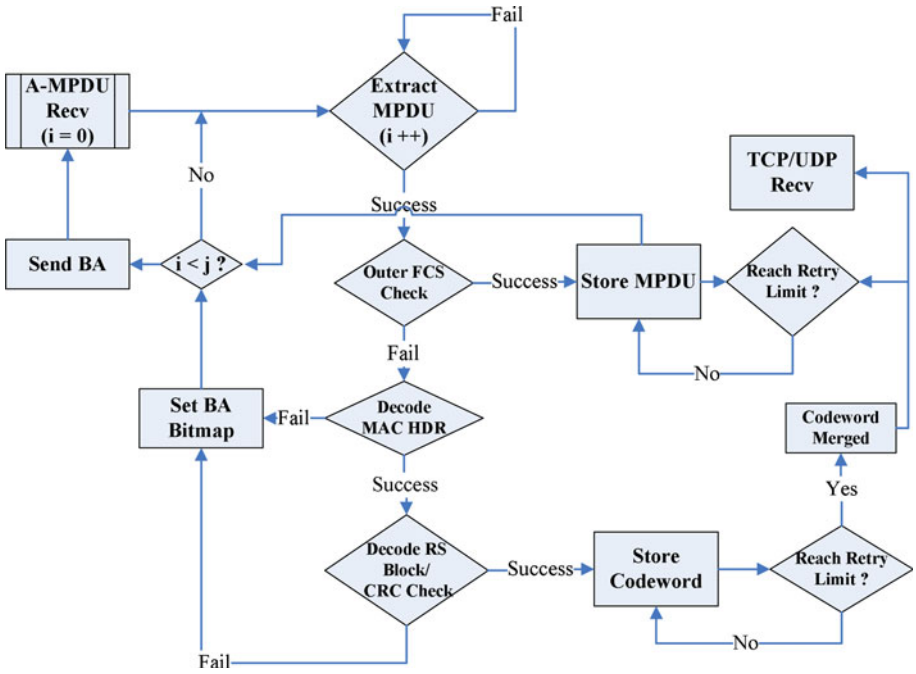

Fig. 2 The flow diagram of retransmission mechanism for proposed AH-ARQ scheme

is to implement the ASR-ARQ algorithm according to the codeword basis. The receiver will store correctable RS blocks and combine these blocks with remaining retrieved correctable RS blocks in order to form a complete new frame. The detail procedures of retransmission mechanism is explained as follows. After the reception of the A-MPDU, Algorithm 2 will be adopted by the receiver to extract each MPDU from the A-MPDU. In the case that the receiver finds errors within a set of RS blocks that are uncorrectable, it will disable the bits within BA frame's bitmap field that map to the corresponding MPDUs. On the other hand, if the RS blocks are either correctly received or with correctable errors, the receiver will enable the corresponding bits in bitmap field of BA frame. The receiver will stores the set of correct RS blocks of the MPDU and the associated header information, including both the sequence number and the retry times of this MPDU. After all the MPDUs of an A-MPDU have been extracted, the receiver will consequently send a BA frame back to the transmitter associated with information specified in its bitmap field. On the transmitter side, retransmission of uncorrectable RS blocks will be determined by observing the disabled bits within the received BA frame's bitmap field. The transmitter will initiate a retransmission of an A-MPDU with each MPDU containing the MAC header's RS block associated with the uncorrectable RS blocks in ascending sequence. Either after all the RS blocks have been correctly received or the retry limit has been reached, the transmitter will continue to deliver remaining A-MPDUs to its corresponding receiver based on similar retransmission mechanism.

3 Unsaturated performance analysis of proposed ARQ schemes

In this section, novel analytical models based on the signal flow graph are exploited to analyze the performance of proposed ASR-ARQ and AH-ARQ mechanisms. A pair of transmitter and receiver with either uplink or downlink unicast transmission is assumed for performance analysis. Unsaturated traffic flows and limited queue with queue length equal to K are considered. Furthermore, the distributed coordination function (DCF) is employed as the medium access scheme for one access category between the transmitter and receiver. The request-to-send/clear-to-send (RTS/CTS) mechanism is used for channel reservation in order to enhance the basic access scheme. Subsection 3.1 describes the queuing model under the unsaturated situation. Analytical models for proposed ASR-ARQ and AH-ARQ schemes are proposed in Subsects. 3.2 and 3.3 respectively. The iterative algorithm for conducting the proposed ARQ mechanisms is presented in Subsect. 3.4.

3.1 Queuing model of frame aggregation

In order to describe the traffic characteristics of IEEE 802.11n MAC protocol for the unsaturated case, a discrete time $M/G^{[\alpha,\beta]}/1/K$ queuing model is adopted in this paper. It is noted that $[\alpha, \beta]$ denotes the integer range for the total number of aggregated packets, and K is the maximum number of packets that can be stored in the queue. An embedded Markov process is considered at the time instant δ_r^- just before the departure of j aggregated packets waiting

in the queue. The transition probability from i to j packets ($j > i$) within the queue can be defined as $p_{ij}^{(s)} = Pr\{x(\delta_r^-) = x_j | x(\delta_{r-s}^-) = x_i\}$. From the properties of ergodic Markov chains, the convergence of transition probability is obtained as $\lim_{s\to\infty} p_{ij}^{(s)} = p_{ij}$. The steady state probabilities are represented as $\pi_j = \lim_{s\to\infty} \pi_j^{(s)} = \lim_{s\to\infty} \sum_i \pi_i^{(0)} \cdot p_{ij}^{(s)} = \sum_i \pi_i^{(0)} \cdot p_{ij}$, which indicates the probability with j packets in the queue. Considering the case with unlimited queue length, i.e. $K \to \infty$, the steady state probability π_j can be obtained as

$$\pi_j = \begin{cases} \kappa_0 \sum_{i=0}^{\beta} \pi_i, & j = 0 \\ \kappa_j \sum_{i=0}^{\beta} \pi_i + \sum_{i=\beta+1}^{\beta+j} \kappa_{\beta+j-i}\pi_i, & j \geq 1 \end{cases} \quad (1)$$

where κ_j for $j \geq 0$ denotes the probability that there are j packets arrived within the service time as

$$\kappa_j = \int_0^{\infty} e^{-\lambda t} \frac{(\lambda t)^j}{j!} dT(t) \quad (2)$$

with λ indicating the packet arrival rate. $T(t)$ represents the cumulative distribution function (CDF) of service time distribution for medium access delay, which will be obtained in the next subsection. On the other hand, considering the case with limited queue length K, the steady state probabilities π_j as in (1) can be modified as

$$\pi_j = \begin{cases} \kappa_0 \sum_{i=0}^{\beta} \pi_i, & j = 0 \\ \kappa_j \sum_{i=0}^{\beta} \pi_i + \sum_{i=\beta+1}^{\beta+j} \kappa_{\beta+j-i}\pi_i, & 1 \leq j < K-\beta \\ \kappa_j \sum_{i=0}^{\beta} \pi_i + \sum_{i=\beta+1}^{K} \kappa_{\beta+j-i}\pi_i, & K-\beta \leq j < K \\ 1 - \sum_{i=0}^{K-1} \pi_i, & j = K \\ 0, & j > K \end{cases} \quad (3)$$

where κ_j can also be acquired from (2). The queuing model with limited queue length in (3) will be utilized for the derivation of unsaturated performance of the proposed ARQ schemes.

3.2 Modeling of service time distribution for proposed ASR-ARQ scheme

The service time distribution for the transmitter can be obtained from the state diagram based on the modified Bianchi's model [26]. As stated in the IEEE 802.11n standard, the time duration for a transmission opportunity (TXOP) indicated by a long NAV (T_{LNAV}) should be large enough to accommodate a typical A-MPDU sequence. In general, T_{LNAV} is suggested to be twice in time duration compared with the time required for the A-MPDUs transmission, i.e. $T_{LNAV} = T_{RTS} + T_{CTS} + 2T_{A-MPDU} + 2T_{BA} + 5T_{SIFS}$ where these parameters are denoted via their corresponding subscripts and T_{SIFS} represents the time duration for a short interframe space. In the case that an A-MPDU is failed in transmission, the second half of T_{NAV} will be utilized for transmitting unsuccessful MPDUs within the A-MPDU. As shown in Fig. 3, the signal flow graph is utilized to depict the characteristics of proposed ASR-ARQ scheme in order to calculate the probability for the MPDUs to be positively acknowledged. Signal flow diagram has been well-adopted in signal processing and control systems to denote the relationship between different variables, which is exploited in this paper to represent the corresponding Markov chain of the proposed scheme. The transition probability $t_{i,j}$ is utilized to indicate the transition from the state that there are i packets left to be transmitted to the state that there are remaining j packets waiting for transmission, i.e.

$$t_{i,j} = \begin{cases} 1, & i = j = 0 \\ C_j^i f_e^j (1-f_e)^{i-j}, & i \geq j \\ 0, & i < j \end{cases} \quad (4)$$

The parameter f_e denotes the frame error probability as $f_e = 1 - (1 - b_e)^{Nb}$, where b_e corresponds to the bit error rate (BER) and N_b is the total number of bits within an MPDU. Based on (4) and the signal flows obtained from Fig. 3, the recurrent function $R_j(D)$ at the jth state that formulates the behaviors of the ASR-ARQ algorithm can be acquired as

$$R_j(D) = \sum_{r=0}^{j} \sum_{s=0}^{r} C_r^j C_s^r (1-f_e)^{j-s} f_e^{r+s} D R_s(D) \quad (5)$$

for $j > 0$, and $R_0(D) = 1$. The parameter D indicates the transition gain as the state changes. The recurrent function $R_j(D)$ represents the summation of all the possibilities for the transition from the jth state to the 0th state, i.e. the probability to finish the transmission of the entire j packets.

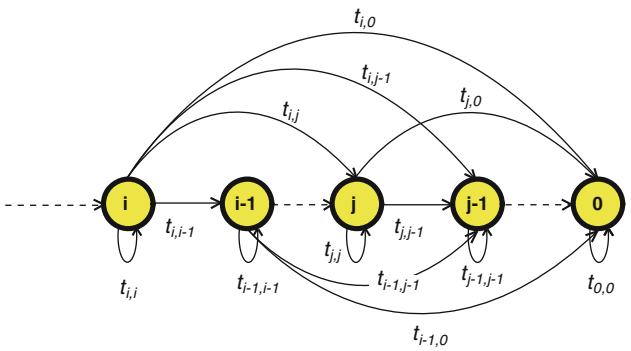

Fig. 3 Signal flow graph for the proposed ASR-ARQ and AH-ARQ schemes

Based on the T_{LNAV} design of proposed ASR-ARQ scheme, an additional retransmission is considered in (5) in the case that an A-MPDU is failed in its original transmission. For example, considering that there is only one packet (i.e. $j = 1$) waiting to be transmitted, the recurrent function becomes $R_1(D) = (1-f_e)DR_0(D) + (1-f_e)f_eDR_0(D) + f_e^2DR_1(D)$ where the three terms respectively denote the probabilities for the original transmission to be successful, a failed original transmission with a successful retransmission, and errors occur in both original transmission and retransmission. It is noted that the first two terms is multiplied by $R_0(D)$ since the packet can finally be successfully transmitted within a single TXOP; while the $R_1(D)$ parameter in the third term indicates that an additional TXOP is required due to the twice unsuccessful transmissions.

In order to solve the recurrent equation as in (5), a transformed function $\tilde{R}(x)$ is defined as

$$\tilde{R}(x) \triangleq \sum_{j=0}^{\infty} R_j(D)\frac{x^j}{j!} \tag{6}$$

By substituting x in (6) with f_e^2x associated with the relationships $e^{(1-f_e)x} = \sum_{j=0}^{\infty}\frac{[(1-f_e)x]^j}{j!}$ and $e^{(1-f_e^2)x} = \sum_{j=0}^{\infty}\frac{[(1-f_e^2)x]^j}{j!}$, $\tilde{R}(x)$ can be acquired as

$$\tilde{R}(x) = D\tilde{R}(f_e^2x)e^{(1-f_e^2)x} + (1-D) \tag{7}$$

By defining $Q(x) \triangleq \frac{\tilde{R}(x)}{e^x}$, $\tilde{R}(x)$ as in (7) can be represented by $Q(x)$ as

$$Q(x) = Q(f_e^2x)D + (1-D)e^{-x} \tag{8}$$

On the other hand, similar to the relationship in (6), $Q(x)$ can also be expressed as

$$Q(x) = \sum_{j=0}^{\infty} Q_j(D)\frac{x^j}{j!} \tag{9}$$

By combining (8) and (9), $Q(x)$ can be obtained as

$$Q(x) = \sum_{j=0}^{\infty}\left[D\frac{(f_e^2x)^j}{j!}Q_j(D) + (-1)^j(1-D)\frac{x^j}{j!}\right] \tag{10}$$

By associating (9) and (10), $\tilde{R}(x)$ can be rewritten as

$$\tilde{R}(x) = e^xQ(x) = \left[\sum_{j=0}^{\infty}\frac{(-1)^j(1-D)x^j}{1-Df_e^{2j} \quad j!}\right]\cdot\sum_{r=0}^{\infty}\frac{x^r}{r!} \tag{11}$$

Finally, $R_j(D)$ can be obtained from (6) to (11) as

$$R_j(D) = \sum_{r=0}^{j!}\frac{j \qquad (-1)^r(1-D)}{(j-r)!r! \quad 1-Df_e^{2r}} \tag{12}$$

The recurrent function $R_j(D)$ derived in (12) implies the mechanism of proposed ASR-ARQ scheme, which will be utilized for the computation of successful transmission probability, i.e. $p_{m,j,0}$. It indicates the probability generating function (PGF) for zero unsuccessful packet that is waiting to be transmitted at the beginning of the mth backoff stage under the initial j aggregated packets. The CDF $p_{m,j,0}$ can be obtained by taking the derivatives of recursion Eq. (12) as

$$p_{m,j,0} = \sum_{s=1}^{m}\left[\frac{1}{s!}\cdot\frac{d^sR_j(D)}{dD^s}\right]_{D=0} \tag{13}$$

It is noted that the sth derivative of (12) indicates that packets are successfully delivered at the $(s-1)$th stage. In other words, the CDF $p_{m,j,0}$ represents that all the packets are successfully transmitted between the 0th and the $(m-1)$th backoff stages.

Moreover, it is noticed that the medium access delay can be divided into two parts, including both the backoff delay and the transmission delay. First of all, the backoff delay is represented by considering the PGF of consecutive backoff time slots defined as $H_d(z) = z^{\sigma}$ with σ denoting the length of a single time slot. Accordingly, the PGF for the backoff delay at the ith stage $H_i(z)$ is obtained as

$$H_i(z) = \begin{cases} \frac{1}{2^iW}\sum_{r=0}^{2^iW-1}H_d^r(z), & 0 \le i < M \\ \frac{1}{2^MW}\sum_{r=0}^{2^MW-1}H_d^r(z), & M \le i \le R_l - 1 \end{cases} \tag{14}$$

where W is the minimum contention window size, R_l indicates the retry limit, and M denotes the maximum number of retransmissions. On the other hand, the transmission delay is composed by both the unsuccessful and the successful transmission time. Considering that there are j aggregated packets within an A-MPDU, the PGF $F_{m,j}(z)$ for unsuccessful transmission between the mth and the $(m+1)$th backoff stages is conditioned based on the followings: (a) $(1-p_{m,j,0})$: the probability that there is at least one packet that is unsuccessfully transmitted before the starting of mth backoff stage; and (b) $\xi_k = 1 - \sum_{r=0}^{k}C_r^kf_e^r(1-f_e)^k$: the probability of at least one packet is failed in transmission within k packets $(k \le j)$ at the current transmission stage. Therefore, the PGF $F_{m,j}(z)$ can be obtained as

$$F_{m,j}(z) = \frac{1}{1-p_{m,j,0}}\sum_{k=1}^{j}\frac{p_{m,j,k}}{\xi_k}\cdot\sum_{r=1}^{k}C_r^kf_e^r(1 - f_e)^{k-r}z^{kT_{\eta_1}+T_1}\sum_{s=1}^{r}C_s^rf_e^s(1-f_e)^{r-s}z^{rT_{\eta_1}+T_2} \tag{15}$$

where $T_1 = T_{RTS} + T_{CTS} + 3T_{SIFS} + T_{BA}$ and $T_2 = 2T_{SIFS} + T_{BA}$. The parameter T_{η_1} in (15) denotes the required transmission time of a single MPDU as $T_{\eta_1} = (n_d \cdot t_s)/n_o$, where n_d represents the number of data bytes per MPDU, t_s

corresponds to the symbol duration, and n_o indicates the number of transmitted data bytes per OFDM symbol duration. The parameter $p_{m,j,k}$ in (15) denotes the probability that there are k unsuccessfully transmitted MPDUs at the mth backoff stage, which can be represented as the $(k+1)$th element of the vector $v^{(m)}_p$, i.e. $p_{m,j,k} = [v_p^{(m)}]_{1,k+1}$. It is noticed that $v_p^{(m)} = v_p^{(0)} \times \mathbf{T}^{2m}$, which corresponds to the multiplication of the initial vector $v_p^{(0)} = [0\ 0\ ...\ 0\ 1]$ and the transition matrix $\mathbf{T}^{2m}$. The elements $t_{i,j}$ within the transition matrix $\mathbf{T}_{(j+1)\times(j+1)}$ can be acquired from (4). Consequently, considering the generic case of $\alpha \le j \le \beta$, the PGF $F_m(z)$ for unsuccessful transmission between the mth and the $(m+1)$th backoff stages becomes

$$F_m(z) = \sum_{j=\alpha}^{\beta} \Pi_j F_{m,j}(z) \tag{16}$$

where the parameter Π_j denotes the PMF of j aggregated packets. It can be obtained as

$$\Pi_j = \begin{cases} \sum_{i=0}^{\alpha} \pi_i, & j = \alpha \\ \pi_j, & \alpha < j < \beta \\ \sum_{i=\beta}^{K} \pi_i, & j = \beta \end{cases} \tag{17}$$

where π_js are acquired from (3) in Subsect. 3.3. A under the case of limited queue length. Moreover, with $\alpha \le j \le \beta$, the PGF $S_m(z)$ for successful transmission time at the mth backoff stage can be obtained as

$$S_m(z) = \sum_{j=\alpha}^{\beta} \frac{\Pi_j}{1-p_{m,j,0}} \sum_{k=1}^{j} \frac{p_{m,j,k}}{\varepsilon_k} \cdot \left[(1-f_e)^k z^{kT_\eta + T_1} + \sum_{r=1}^{k} C_r^k f_e^r (1-f_e)^k z^{(k+r)T_\eta + T_3} \right] \tag{18}$$

where $T_3 = T_{RTS} + T_{CTS} + 5T_{SIFS} + 2T_{BA}$. The parameter $\varepsilon_k = 1 - \sum_{r=1}^{k} \sum_{s=1}^{r} C_r^k C_s^r f_e^{r+s} (1-f_e)^{k-s}$ denotes the probability that a total of k packets are successfully transmitted, where $k \le j$. As a consequence, the overall PGF $T(z)$ of the service time distribution can be formulated by combining (14), (16), and (18) as

$$T(z) = (1-\psi_0) z^{T_{DIFS}} H_0(z) S_0(z) + \prod_{i=0}^{R_l-1} z^{T_{DIFS}} H_i(z) \times \prod_{m=0}^{R_l-1} \psi_m F_m(z) + \sum_{i=1}^{R_l-1} \prod_{r=0}^{i} z^{T_{DIFS}} H_r(z) \prod_{m=0}^{i-1} \psi_m F_m(z) \times (1-\psi_i) S_i(z) \tag{19}$$

where $\psi_m = \sum_{j=\alpha}^{\beta} \Pi_j \sum_{k=1}^{j} p_{m,j,k} \xi_k$. It represents the failed transmission probability at the mth stage and will continue to the $(m+1)$th stage for transmission, where $0 \le m \le R_l - 1$.

3.3 Modeling of service time distribution for proposed AH-ARQ scheme

In this section, the performance analysis and modeling for the service time distribution of proposed AH-ARQ scheme is presented. Based on the RS code, the decoding errors occur while there are more than τ corrupted symbols within a predefined block. Therefore, a decoding error probability B of a block can be formulated as

$$B = \sum_{r=\tau+1}^{n_c} C_r^{n_c} s_e^r (1-s_e)^{n_c - r} \tag{20}$$

where the codeword length $n_c = 2^{n_b} - 1$ as defined in Subsect. 2.3.1. The parameter s_e represents the error rate of an RS symbol defined in $GF(2^{n_b})$ with n_b bits, i.e. $s_e = 1 - (1-b_e)^{n_b}$ where b_e corresponds to the BER as defined in Subsect. 3.2. It is noticed that B as defined in (20) is usually served as an upper bound of decoding errors for the RS code. By adopting the same signal flow graph as in Fig. 3 for the AH-ARQ mechanism, the parameter $t_{i,j}$ is renamed as $t'_{i,j}$ for clarity to represent the transition probability from the state with i remaining packets to the state that there are j packets to be transmitted. The value of $t'_{i,j}$ can be obtained as

$$t'_{i,j} = \begin{cases} 1, & i = j = 0 \\ h_e + (1-h_e)B^i, & 1 \le i \le n_r,\ j = i \\ C_j^i (1-h_e) B^j (1-B)^{i-j}, & 0 \le j < i \\ 0, & i < j \end{cases} \tag{21}$$

where $n_r = \lceil L_{MPDU}/n_c \rceil$ denotes the total number of RS codewords in an MPDU with L_{MPDU} representing the total number of symbols in an MPDU. The parameter h_e represents the union of error probabilities from both the packet header and the delimiter. It is noticed that if the value of h_e is greater than zero, the entire MPDU will be retransmitted. According to (21) and Fig. 3, the recurrent function $R_j(D)$ at the jth state defined for the proposed AH-ARQ scheme to transmit A-MPDUs in one TXOP channel reservation can be reformulated as

$$R_j(D) = h_e^2 D R_j(D) + 2h_e(1-h_e)D \sum_{k=0}^{j} C_k^j B^k (1-B)^{j-k} R_k(D) + (1-h_e)^2 D \sum_{r=0}^{j} \sum_{s=0}^{r} C_r^j C_s^r B^{r+s} (1-B)^{j-s} R_s(D) \tag{22}$$

for $1 \le j \le n_r$, and $R_0(D) = 1$. In order to represent the case for an MPDU composed of n_r RS blocks under error-prone channels, similar procedures as described in (6–12) are adopted for solving the recurrent relationship. The recurrent function $R_j(D)$ can therefore be acquired as

$$R_j(D) = \sum_{r=0}^{j} \frac{j!}{(j-r)!r!} \cdot \frac{(D-1)(-1)^r}{2Dh_e(1-h_e)B^r + D(1-h_e)^2B^{2r} - (1-Dh_e^2)} \tag{23}$$

for $1 \le j \le n_r$. Consequently, the behavior of retransmission mechanism for an MPDU consists of n_r RS blocks with under error-prone channel can be depicted. It is noted that the recurrent function $R_j(D)$ obtained from (23) is merely applied for a single MPDU. The case with j MPDUs that are aggregated in an A-MPDU is considered as follows. A discrete random variable X is utilized to indicate the number of transmission retries until all the RS blocks of an A-MPDU have been positively acknowledged. Similar to the concept as adopted in (13), the probability density function of X at the mth backoff stage can be represented as

$$P_X(m) = \left[\sum_{s=1}^{m} \frac{1}{s!}\frac{d^s R_{n_r}(D)}{dD^s}\right]^j u(m) - \left[\sum_{s=1}^{m-1} \frac{1}{s!}\frac{d^s R_{n_r}(D)}{dD^s}\right]^j u(m-1) \tag{24}$$

where $u(m) = 1$ if $m > 0$ and $u(m) = 0$ for $m \le 0$. It is noted that the derivative is performed at $R_{n_r}(D)$ since each MPDU has n_r codewords. Based on (24), the CDF $p'_{m,j,0}$ for all packets to be successful transmitted before the mth transmission retry can be obtained by solving the following relationship:

$$P_X(m) = (p'_{m,j,0})^j u(m) - (p'_{m-1,j,0})^j u(m-1) \tag{25}$$

Noted that the value of CDF $p'_{m,j,0}$ by adopting the AH-ARQ protocol will be evaluated by comparing both the analytical and simulation results in Sect. 4. In order to calculate the service time distribution of proposed AH-ARQ scheme, both the PGFs for the failed transmission $F_{m,j,n_r}(z)$ and the successful transmission $S_{m,j,n_r}(z)$ are required to be obtained first. Consider the jth packet in an A-MPDU, the PGF of failed transmission time $F_{m,j,n_r}(z)$ at the mth backoff stage is formulated as

$$F_{m,j,n_r}(z) = \sum_{k=1}^{n_r} \frac{p'_{m,j,k}}{(1-p'_{m,j,0})\xi'_k} \cdot z^{\frac{T_3}{j}+2T_m+kT_{\eta_2}} \times \left[h_e^2 z^{kT_{\eta_2}} + (1-h_e)h_e \sum_{r=1}^{k} C_r^k B^r (1-B)^{k-r} \cdot (z^{rT_{\eta_2}} + z^{kT_{\eta_2}}) + (1-h_e)^2 \sum_{r=1}^{k}\sum_{l=1}^{r} C_r^k C_l^r (1-B)^{k-l} B^{r+l} z^{rT_{\eta_2}}\right] \tag{26}$$

where $\xi'_k = 1 - (1-h_e^2)(1-B)^k - (1-h_e)^2 \sum_{r=1}^{k} C_r^k B^r (1-B)^k$. The parameter $T_3 = T_{RTS} + T_{CTS} + 5T_{SIFS} + 2T_{BA}$ is the same as defined in (18). Noted that the computation of $(2T_{BA} + 3T_{SIFS})/j$ is an approximated value for the time duration of common control packets. The parameter T_{η_2} represents the time interval for each RS block transmission; while T_m corresponds to the time duration of MAC header utilized by the codewords. Furthermore, $p'_{m,j,k}$ in (26) indicates the probability of k unsuccessfully received RS blocks after m retransmissions which can be represented as the $(k+1)$th element of the vector $v'^{(m)}_p$, i.e. $p_{m,j,k} = [v'^{(m)}_p]_{1,k+1}$. Noted that $v'^{(m)}_p = v'^{(0)}_p \times (\mathbf{T}')^{2m}$ corresponds to the multiplication of initial vector $v'^{(0)}_p = [0\,0 \ldots 0\,1]$ and transition matrix $(\mathbf{T}')^{2m}$ for each transmission opportunity. The elements $t'_{i,j}$ in the transition matrix $\mathbf{T}'_{(n_r+1)\times(n_r+1)}$ can be obtained from (21). On the other hand, consider the jth packet within an A-MPDU, the successful transmission time at the mth backoff stage is depicted as

$$S_{m,j,n_r}(z) = \sum_{k=1}^{n_r} \frac{p'_{m,j,k}}{(1-p'_{m,j,0})\varepsilon'_k} \cdot z^{\frac{T_4}{j}} \Big[(1-h_e)(1-B)^k z^{T_m+kT_{\eta_2}+\frac{T_5}{j}} + h_e(1-h_e)(1-B)^k z^{2T_m+2kT_{\eta_2}+\frac{T_6}{j}} + (1-h_e)^2 \sum_{l=1}^{k} C_l^k B^l (1-B)^k z^{2T_m+(k+l)T_{\eta_2}+\frac{T_6}{j}}\Big] \tag{27}$$

where $T_4 = T_{RTS} + T_{CTS} + 2T_{SIFS}, T_5 = T_{SIFS} + T_{BA}$, and $T_6 = 3T_{SIFS} + 2T_{BA}$. The parameter $\varepsilon'_k = 1 - h_e^2 - 2(1-h_e)h_e \sum_{r=1}^{k} C_r^k B^r (1-B)^{k-r} - (1-h_e)^2 \sum_{r=1}^{k}\sum_{s=1}^{r} C_r^k C_s^r B^{r+s}(1-B)^{k-s}$ indicates the probability that there are k successfully transmitted packets with $k \le j$. Therefore, the PGF of service time distribution for a single jth packet can be obtained as

$$T_{j,n_r}(z) = (1-\psi'_0) z^{T_{DIFS}} H_0(z^{j-1}) S_{0,j,n_r}(z) + \sum_{i=1}^{R_l-1} (1-\psi'_i) S_{i,j,n_r}(z) \cdot \tag{28}$$

$$\left[\left(\prod_{l=0}^{i} z^{T_{DIFS}} H_l(z^{j-1})\right)\left(\prod_{m=0}^{i-1} \psi'_m F_{m,j,n_r}(z)\right)\right] + \prod_{i=0}^{R_l-1} z^{T_{DIFS}} H_i(z^{j-1}) \prod_{m=0}^{R_l-1} \psi'_m F_{m,j,n_r}(z) \quad (29)$$

where ψ'_m represents the failed transmission probability for an MPDU containing n_r RS blocks, i.e. $\psi'_m = \sum_{k=1}^{n_r} p'_{m,j,k}\xi'_k$, and $H_l(z^{j-1})$ is obtained from (14) by substituting z with z^{j-1}. As a result, the PGF $T_{n_r}(z)$ of service time distribution for the entire A-MPDU by aggregating j from α to β can be obtained as

$$T_{n_r}(z) = \sum_{j=\alpha}^{\beta} \Pi_j \cdot [T_{j,n_r}(z)]^j \quad (30)$$

where Π_j is acquired from (17). The validation and comparison for the service time distribution $T_{n_r}(z)$ will be performed in Sect. 4.

3.4 Iterative algorithm for proposed ASR-ARQ and AH-ARQ schemes

In order to calculate the service time distributions as in (19) and (30) for the proposed ASR-ARQ and AH-ARQ schemes respectively, an iterative algorithm is required to be exploited. The reason for the usage of iterative method is that the service time distributions in (19) and (30) are functions of steady state probability π_j in (3), which is derived from κ_j as the probability that there are j packets arrived within the service time. However, it can be observed from (2) that κ_j is a function of service time distribution. Therefore, it is required to utilize the iterative process in order to obtain the service time distributions. The procedures of the iterative algorithm are listed as follows:

1. The algorithm starts with the initial condition of saturation case, i.e. $[\pi_0\pi_1 \ldots \pi_{K-1}\pi_K] = [00\ldots01]$.
2. Calculate the service time distribution of either PGF $T(z)$ in (19) for the ASR-ARQ scheme or PGF $T_{n_r}(z)$ in (30) for the AH-ARQ algorithm.
3. It is assumed that 1 μs is taken as the sampling interval for the iterative algorithm. From the PGF $T(z)$ as in (19) (or $T_{n_r}(z)$ in (30)), its corresponding PMF $\mathcal{T}_i$ can consequently be obtained which denotes the probability that the service time is i μs. Based on the acquisition of $\mathcal{T}_i$, the probability κ_j as defined in (2) can be approximated and obtained as $\kappa_j \simeq \sum_{i=0}^{\infty} \mathcal{T}_i e^{-\lambda i} \frac{(\lambda i)^j}{j!}$. By substituting the probability κ_j into (3), the newly updated steady state probability vector $[\pi'_0\pi'_1 \ldots \pi'_{K-1}\pi'_K]$ can therefore be acquired.
4. Based on the updated π'_j obtained from step 3, a new service time distribution $T'(z)$ can be recalculated via (19) (or $T'_{n_r}(z)$ in (30)). The newly acquired PMF $\mathcal{T}'_i$ will be compared with the previously computed $\mathcal{T}_i$ value that was obtained from step 2. In the case that the difference between these two values are within a pre-specified threshold, the iterative process will be terminated. If not, the iterative procedure will be continued and proceed from step 2.

4 Performance evaluation

In this section, the performance of proposed ASR-ARQ and AH-ARQ schemes will be validated and compared via simulations. The binary symmetric channel is assumed for performance comparison under error-prone channels. A system C/C++ network simulation model is constructed by considering the access point (AP) based single-hop communications. As shown in Table 1, the MAC-defined parameters that are described in the IEEE 802.11n standard is adopted in both the analytical models and the simulations.

The validation of proposed analytical models for both the ASR-ARQ and AH-ARQ schemes are illustrated from Figs. 4, 5, 6, and 7. For validation purpose, an AP and a single user station is considered within the network. Fig. 4 shows the validation for the ASR-ARQ scheme via the successful transmission probability $p_{m,j,0}$ obtained from (13) versus the number of retransmission stage m. Each A-MPDU is aggregated with 10 MPDUs, i.e. $j = 10$; while the size of each MPDU is configured as 1024 bytes. Four different channel conditions are considered for model validation, i.e. BER $b_e = 5 \times 10^{-5}, 10^{-4}, 2 \times 10^{-4}$, and 2.5×10^{-4}. The results obtained from the analytical model are denoted as "ana"; while that from the simulations are represented as "sim". It can be observed that the results

Table 1 Parameters for performance evaluation

Parameter	Value
RTS packet size	20 Bytes
CTS packet size	14 Bytes
Block ACK (BA) packet size	32 Bytes
MAC header size	28 Bytes
Time duration of *DIFS* (T_{DIFS})	34 μs
Time duration of *SIFS* (T_{SIFS})	16 μs
Length of single time slot (σ)	9 μs
Retry_Limit (R_l)	7
Minimum contention window size (W)	8
Maximum number of retransmission (M)	7
Data rate	24 Mbps

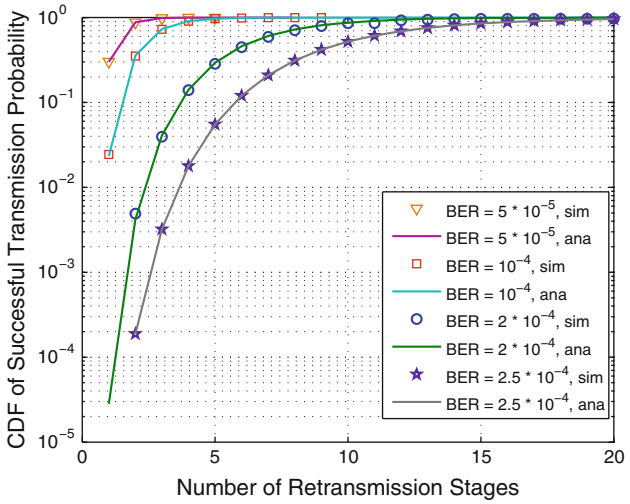

Fig. 4 Performance validation for ASR-ARQ scheme: successful transmission probability $p_{m,j,0}$ versus number of retransmission stage (m)

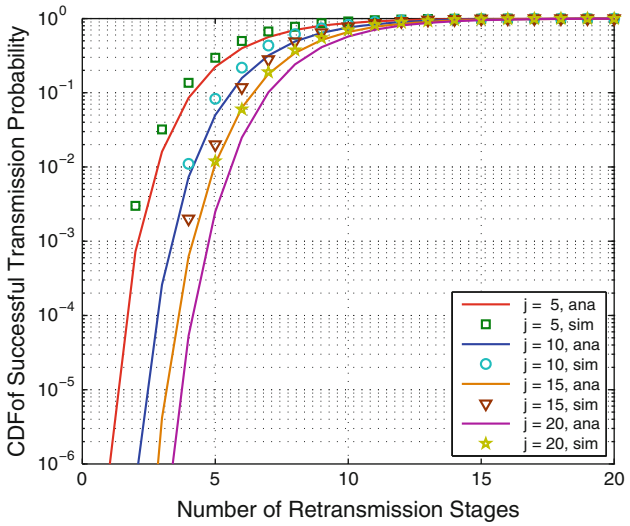

Fig. 5 Performance validation for AH-ARQ scheme: successful transmission probability $p'_{m,j,0}$ versus number of retransmission stage (m)

from both the analytical model and the simulations are consistent with each other under the various BER values. The successful transmission probability $p_{m,j,0}$ is increased as the BER value is decremented. Furthermore, with a larger number of the backoff stage m, it is reasonable to find that higher value of successful transmission probability can be obtained. On the other hand, Fig. 5 illustrates the successful transmission probability $p'_{m,j,0}$ in (25) from AH-ARQ algorithm versus the number of retransmission stage m under BER $b_e = 10^{-2}$. Four different aggregation sizes are considered including $j = 5$, 10, 15 and 20. The (255,223,16) RS code over $GF(2^8)$ is constructed for the proposed AH-ARQ scheme via the primitive polynomial

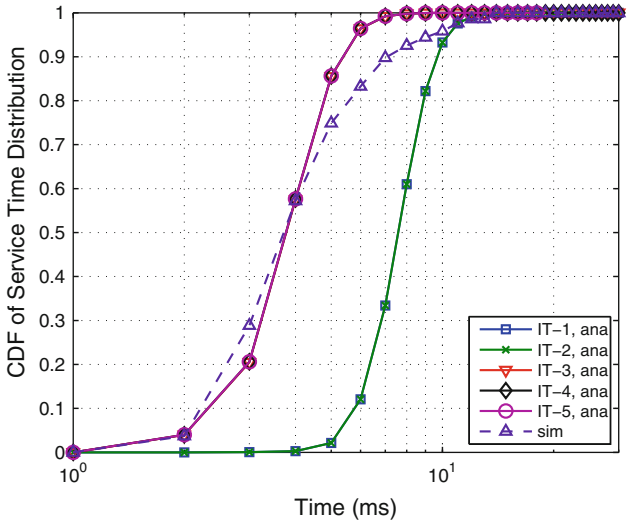

Fig. 6 Performance validation for ASR-ARQ scheme: service time distribution $T(z)$ under different numbers of iterations

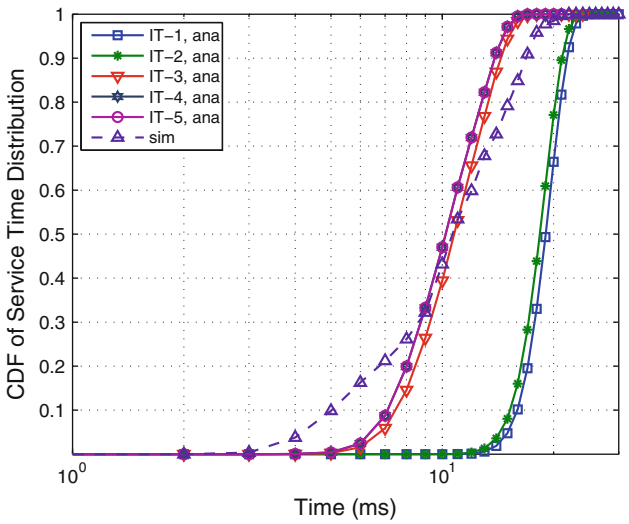

Fig. 7 Performance validation for AH-ARQ scheme: service time distribution $T_{n_r}(z)$ under different numbers of iterations

$1 + x^2 + x^3 + x^4 + x^8$. Each 835-bytes MPDU within an A-MPDU consists of three RS blocks which excludes the header and delimiter blocks. It is observed that there exists slight discrepancies between the analytical and simulation results. The analytical results will have smaller successful transmission probability comparing with that from the simulation results due to the adoption of upper bound for the decoding error probability B as defined in (20). Furthermore, it is intuitive to find from Fig. 5 that larger number of packet aggregation will result in excessive number of retransmission stages.

Figures 6 and 7 respectively show the model validation for service time distribution $T(z)$ in (19) and $T_{n_r}(z)$ in (30) under different numbers of iterations. The iterative

algorithm as presented in Subsect. 3.4 is utilized for obtaining the proposed analytical models to be compared with the simulation results. The number of aggregated packets varies within the range of $[\alpha, \beta] = [5, 10]$ according the minimum batch rule, the arrival rate λ is set to 100 fps, and the channel condition is chosen as BER $b_e = 2 \times 10^{-4}$. It can be observed from both figures that the service time distributions obtained from the simulations and analytical models are close with each other after several iterations. The iterative process is converged after the third iteration for the ASR-ARQ scheme, i.e. the analytical results for IT =3,4, and 5 are overlapped as in Fig. 6. On the other hand, the recursive process for the AH-ARQ algorithm converges after the fourth iteration as shown in Fig. 7. The slight differences between the simulation and the analytical results can be explained from both the approximation of several parameters and the assumption of Markov ergodic process within the adopted queuing models.

Figures 8 and 9 illustrate the performance comparison for the mean service time and the normalized throughput under different BER values respectively. It is noticed that the mean service time is computed as the averaged value from the service time distribution $T(z)$ in (19) and $T_{n_r}(z)$ in (30) for the proposed ASR-ARQ and AH-ARQ scheme, respectively. The normalized throughput is defined by dividing the throughput with the data rate, i.e. 24 Mbps in this case, where the throughput is designed as the total number of successfully received information bytes within the duration of mean service time. An aggregated stop-and-wait ARQ (ASW-ARQ) scheme is also implemented in the simulations for comparison purpose. It is noticed that the

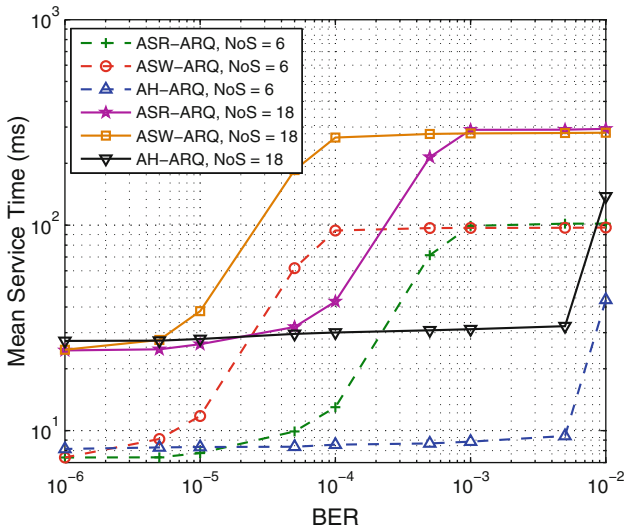

Fig. 8 Performance comparison: mean service time (ms) versus BER values (10 aggregated data units)

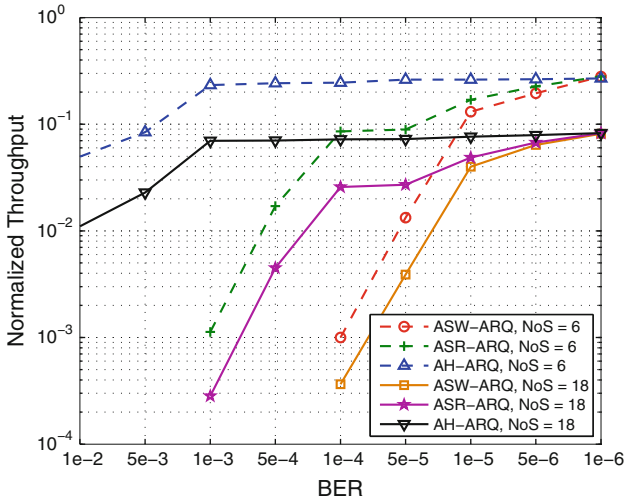

Fig. 9 Performance comparison: normalized throughput versus BER values (10 aggregated data units)

ASW-ARQ approach is equivalent to adopting an ARQ scheme within the aggregated MAC service data unit (A-MSDU). As is defined in the IEEE 802.11n standard, an A-MSDU indicates that an MPDU is composed by multiple MSDUs, where a common CRC check and a MAC header are shared by all the MSDUs within an A-MSDU. For the purpose of fair comparison, the information payload is designed as 657 bytes for all the three algorithms; while 10 data units are aggregated in these schemes, i.e. 10 MPDUs for both the ASR-ARQ and AH-ARQ algorithms and 10 MSDUs for the ASW-ARQ scheme. Two different numbers of stations, i.e. NoS = 6 and 18, are simulated to contend for the channel in order to communicate with the AP. It can be observed from both figures that the proposed AH-ARQ scheme outperforms the ASR-ARQ and ASW-ARQ algorithms under different BER values and numbers of contending stations. Persistent lowered mean service time can be achieved by adopting the AH-ARQ scheme up to BER $b_e = 5 \times 10^{-3}$; while that from the other two algorithms increase significantly for BER value greater than $b_e = 5 \times 10^{-6}$. On the other hand, the normalized throughput for the AH-ARQ method can be retained up to $b_e = 10^{-3}$; while that from the other two schemes decrease drastically after the BER value is larger than $b_e = 10^{-5}$. It is noted that the inferior performance resulting from the ASR-ARQ and ASW-ARQ algorithms is primarily caused by excessive failed retransmissions from packet collisions. Moreover, as shown in Fig. 8, since comparably longer contention period and more collision probabilities can occur, additional access time will be required in all three schemes while there exists more stations contending in the network. The throughput performance will therefore be decreased with the case of NoS = 18 comparing to that with NoS = 6 as shown in Fig. 9.

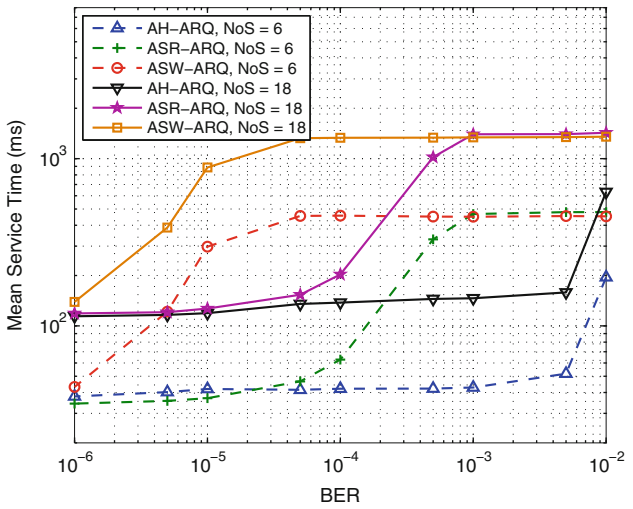

Fig. 10 Performance comparison: mean service time (ms) versus BER values (50 aggregated data units)

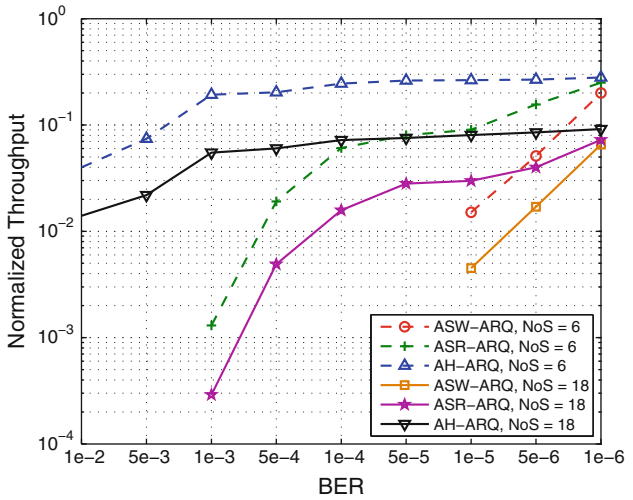

Fig. 11 Performance comparison: normalized throughput versus BER values (50 aggregated data units)

Figures 10 and 11 shows the performance comparison for both the mean service time and normalized throughput with 50 aggregated data units. Noted that a total of 50 MPDUs are aggregated for both the ASR-ARQ and AH-ARQ schemes; while 50 MSDUs is utilized for the ASW-ARQ algorithm. Similar performance results can be obtained from Figs. 10 and 11 comparing with Figs. 8 and 9 respectively. Compared to the other methods, the proposed AH-ARQ scheme can achieve lowered mean service time and higher normalized throughput. It is worthwhile to notice that there is no definite superiority on throughput performance with the increased number of aggregated data units. By observing Figs. 9 and 11, both the ASR-ARQ and ASW-ARQ algorithms result in worse normalized throughput under the case with 50 aggregated data units compared to that with 10 aggregated data units, e.g. under the cases with $b_e = 10^{-5}$ and $b_e = 5 \times 10^{-6}$. The reason can be explained from the tradeoff between the access delay and the effective transmitted information payloads. With larger number of aggregated data units, longer transmission time will be required which results in elongated mean service time. Therefore, by adopting the ASR-ARQ and ASW-ARQ schemes, it is required to investigate the feasibility of increased number of aggregated data units in order to promote the throughput performance under various BER conditions. On the other hand, elongated transmission delay associated with larger number of aggregated MPDUs does not have severe impact on the throughput performance for the AH-ARQ scheme. Based on its adoption of FEC technique, retransmission probability can be reduced which effectively enhances the normalized throughput of AH-ARQ algorithm. The merits of the proposed AH-ARQ scheme can therefore be observed.

5 Conclusion

In this paper, two ARQ mechanisms are proposed with the consideration of frame aggregation under the IEEE 802.11n networks. The aggregated selective repeat ARQ (ASR-ARQ) protocol is proposed by incorporating the conventional selective repeat ARQ scheme; while the aggregated hybrid ARQ (AH-ARQ) algorithm further enhances throughput performance by adopting the Reed-Solomon block code for error correction. Analytical models based on signal flow graph are constructed to evaluate the performance of proposed ASR-ARQ and AH-ARQ algorithms. Simulations are also conducted to validate and compare the effectiveness of proposed ARQ mechanisms via both the mean service time and throughput performance. Numerical results show that the proposed AH-ARQ protocol can outperform the other retransmission schemes under different network scenarios.

Acknowledgment This work was in part funded by the Aiming for the Top University and Elite Research Center Development Plan, NSC 99-2628-E-009-005, NSC 98-2221-E-009-065, the MediaTek research center at National Chiao Tung University, the Universal Scientific Industrial (USI) Co., and the Telecommunication Laboratories at Chunghwa Telecom Co. Ltd, Taiwan.

References

1. IEEE 802.11 WG. (2003). *IEEE Std 802.11a-1999 (R2003): Part 11: Wireless LAN Medium Access Control (MAC) and Physical Layer (PHY) specifications: High-speed physical layer in the 5 GHz Band*. IEEE Standards Association Std.
2. IEEE 802.11 WG. (2003). *IEEE Std 802.11b-1999 (R2003): Part 11: Wireless LAN Medium Access Control (MAC) and Physical*

Layer (PHY) specifications: Higher-speed physical layer extension in the 2.4 GHz Band. IEEE Standards Association Std.
3. IEEE 802.11 WG. (2003). *IEEE Std 802.11g-2003: Part 11: Wireless LAN Medium Access Control (MAC) and Physical Layer (PHY) specifications: Amendment 4: Further higher data rate extension in the 2.4 GHz Band*. IEEE Standards Association Std.
4. IEEE 802.11 WG. (2005). *IEEE Std 802.11e-2005: Part 11: Wireless LAN Medium Access Control (MAC) and Physical Layer (PHY) specifications: Amendment 8: Medium Access Control (MAC) quality of service enhancements*. IEEE Standards Association Std.
5. IEEE 802.11 WG. (2007). *IEEE P802.11n/D3.00: Part 11: Wireless LAN Medium Access Control (MAC) and Physical Layer (PHY) specifications: Amendment 4: Enhancements for higher throughput*. IEEE Standards Association Std.
6. Abraham, S., Meylan, A., & Nanda, S. (2005). 802.11n MAC design and system performance. In *Proceedings of the IEEE international conference on communications (ICC)* (vol. 5).
7. Li, Y., Kim, S. W., Chung, J. K., & Ryu, H. G. (2006). SFBC-based MIMO OFDM and MIMO CI-OFDM systems in the nonlinear and nbi channel. In *Proceedings of the IEEE communications, circuits and systems* (vol. 2. pp. 898–901).
8. Li, Y., Wang, X., & Mujtaba, S. A. (2004). Impact of physical layer parameters on the MAC throughput of IEEE 802.11 wireless LANs. In *Proceedings of the IEEE signals, systems and computers conference* (vol. 2, pp. 1468–1472).
9. Skordoulis, D., Qiang, N., Chen, H. H., Stephens, A. P., Liu, C., & Jamalipour, A. (2008). IEEE 802.11n MAC frame aggregation mechanisms for next-generation high-throughput WLANs. In *IEEE Transactions of Wireless Communications* (vol. 15, pp. 40–47).
10. Ginzburg, B., & Kesselman, A. (2007). Performance analysis of A-MPDU and A-MSDU aggregation in IEEE 802.11n. In *Proceedings of the IEEE Sarnoff symposium*.
11. Parthasarathy, S., & Zeng, Q. -A. (2007). A novel adaptive scheme to improve the performance of the IEEE 802.11n WLANs. In: *Proceedings 21st international conference on advanced Information networking and applications workshops (AINAW)* (vol. 2).
12. Kim, S., Choi, S., Kim, Y., & Jang, K. (2008) MCCA: A high-throughput MAC strategy for next-generation WLANs. *IEEE Wireless Communication of Magazine, 15*, 32–39.
13. Lu, D. L., & Chang, J. F. (1989). Analysis of ARQ protocols via signal flow graphs. *IEEE Transactions of Communication, 37*, 245–251.
14. Hua, Y., & Niu, Z. (2007). An analytical model for IEEE 802.11 WLANs with NAK-based ARQ mechanism. In *Proceedings of the APCC on Communications*.
15. Seo, J. B., Park, N. H., Lee, H. W., & Cho, C. H. (2006). Impact of an ARQ scheme in the MAC/LLC layer on upper-layer packet transmissions over a Markovian channel. In *Proceedings of the IEEE 63rd vehicular technology conference* (vol. 4).
16. Beh, K. C., Doufexi, A., & Armour, S. (2007). Performance evaluation of hybrid ARQ schemes of 3GPP LTE OFDMA system. In *Proceediings of the IEEE 18th personal, indoor and mobile radio communications*.
17. Malkamaki, E., Mathew, D., & Hamalainen, S. (2001). Performance of hybrid ARQ techniques for WCDMA high data rates. In *Proceedings IEEE 53rd vehicular technology conference* (vol. 4. pp. 2720–2724)
18. Wong, T. F., Gao, L., & Lok, T. M. (2001). A type-I hybrid ARQ protocol over optimal-sequence CDMA link. In *Proceedings of the IEEE 21st century military communications* (vol. 1, pp. 559–563).
19. Cheng, J. F., Wang, Y. P. E., & Parkvall, S. (2003). Adaptive incremental redundancy [WCDMA systems]. In *Proceedings IEEE 58th vehicular technology conference* (vol. 2).
20. Chen, Q., Fan, P. (2003). On the performance of type-III hybrid ARQ with RCPC codes. In *Proceedings of the IEEE personal, indoor and mobile radio communications* (vol. 2, pp. 1297–1301).
21. Guo, R., & Liu, J. L. (2006). BER performance analysis of RCPC encoded MIMO-OFDM in Nakagami-m channels. In *Proceedings IEEE information acquisition conference*.
22. Rowitch D. N., & Milstein L. B. (2000) On the performance of hybrid FEC/ARQ systems using RCPT codes. *IEEE Transactions of Communications, 48*, 269–281.
23. Proakis J. G. (2001). *Digital communications*. (4th ed). New York: McGraw-Hill
24. Cheng, U. (1984). On the continued fraction and Berlekamp's algorithm. *IEEE Transactions of Information Theory, 30*, 541–544.
25. Khan, M. A., Afzal, S., & Manzoor, R. (2003). Hardware implementation of shortened (48, 38) Reed Solomon forward error correcting code. In *Proceedings of INMIC multi topic conference*.
26. Bianchi G. (2000). Performance analysis of the IEEE 802.11 distributed coordination function. *IEEE Journal of Selection Areas Communication, 18*, 535–547.
27. Tickoo, O., & Sikdar, B. (2004). Queueing analysis and delay mitigation in IEEE 802.11 random access MAC based wireless networks. In *Proceedings of IEEE INFOCOM*, vol. 2, pp. 1404–1413.
28. Zheng, Y., Lu, K., Wu, D., & Fang, Y. (2005). Performance analysis of IEEE 802.11 DCF in binary symmetric channels. In *Proceedings of IEEE global telecommunications conference*, vol. 5, pp. 3144–3148.
29. Lin, Y., & Wong, V. W. S. (2006). Frame aggregation and optimal frame size adaptation for IEEE 802.11n WLANs. In *Proceedings of IEEE global telecommunications conference*, vol. 5, pp. 1–6.
30. Kuppa, S., & Dattatreya, G. R. (2006). Modeling and analysis of frame aggregation in unsaturated WLANs with finite buffer stations. In *Proceedings of IEEE international conference on communications*.
31. Liu, C. W., & Stephens, A. P. (2005). An analytic model for infrastructure WLAN capacity with bidirectional frame aggregation. In *Proceedings of IEEE wireless communications and networking conference*, vol. 1, pp. 113–119.
32. Berlekamp, E. (1968). *Algebraic coding theory*. New York: McGraw-Hill.

Author Biographies

Kai-Ten Feng received the B.S. degree from National Taiwan University, Taipei, in 1992, the M.S. degree from the University of Michigan, Ann Arbor, in 1996, and the Ph.D. degree from the University of California, Berkeley, in 2000. Since August 2007, he has been with the Department of Electrical Engineering, National Chiao Tung University, Hsinchu, Taiwan, as an associate professor. He was an assistant professor with the same department between February 2003 and July 2007. He joined the Department of Electrical and Computer Engineering, University of California at Davis as a visiting

professor between July 2009 and March 2010. He was with the OnStar Corp., a subsidiary of General Motors Corporation, as an in-vehicle development manager/senior technologist between 2000 and 2003, working on the design of future Telematics platforms and the in-vehicle networks. His current research interests include wireless broadband networks, cooperative and cognitive networks, mobile ad hoc and sensor networks, embedded system design, wireless location technologies, and Intelligent Transportation Systems (ITSs). He received the Best Paper Award from the IEEE Vehicular Technology Conference Spring 2006, which ranked his paper first among the 615 accepted papers. He is also the recipient of the Outstanding Young Electrical Engineer Award in 2007 from the Chinese Institute of Electrical Engineering (CIEE). He has served on the technical program committees of VTC, ICC, and WCNC.

Yu-Zhi Huang received the B.S. degree in electrical engineering from National Tsing Hua University, Taiwan, in 2006. He obtained the M.S. degree in the department of communication engineering at National Chiao Tung University, Taiwan, in 2008. He is currently working for Holtek Semiconductor Inc. in Taipei, Taiwan. His research interests include MAC protocol design in WLAN systems, cross layer optimization, error control techniques, and the implementation of multicast routing protocols.

Jia-Shi Lin received the B.S. degree from National Tsing Hua University, Hsinchu, Taiwan, in 2007. Since 2007, he has been pursuing the Ph.D. degree in the Department of Electrical Engineering, National Chiao Tung University, Hsinchu, Taiwan. His current research interests include game theory, MAC protocol design, wireless local area networks, and cognitive radio networks.